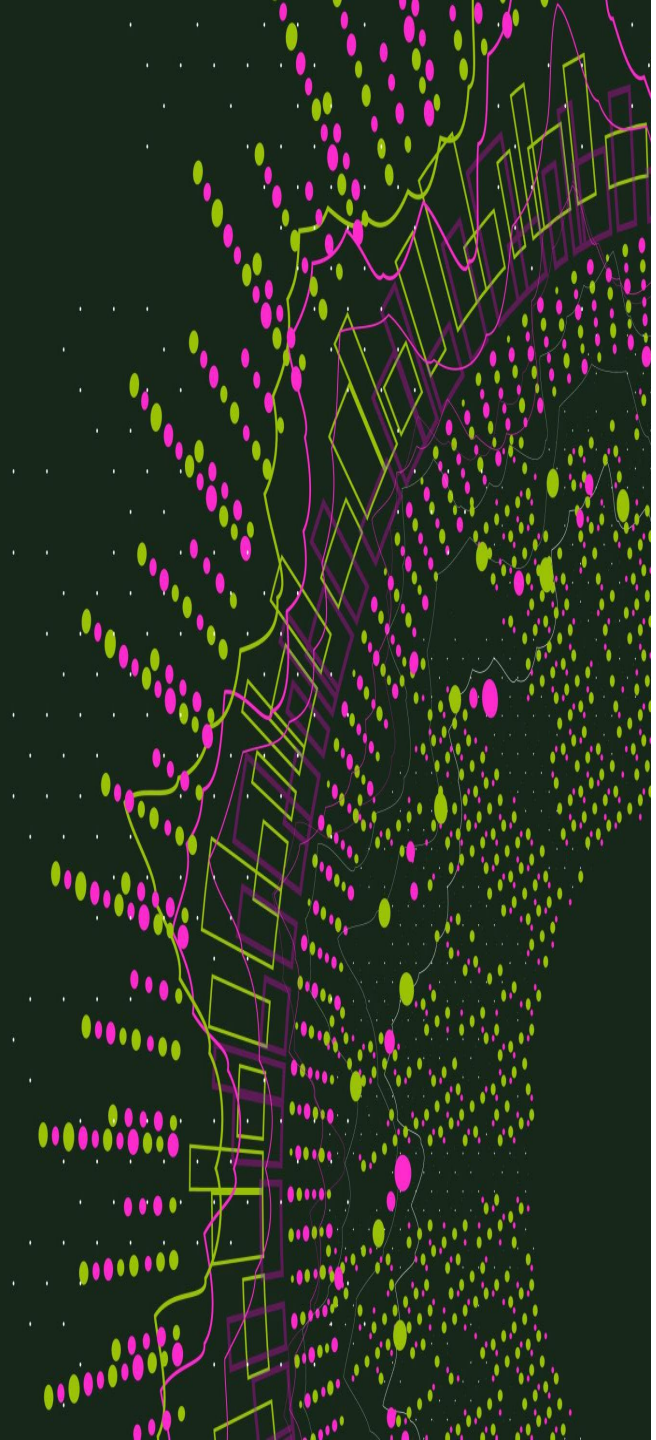

Workshop | Low-energy nuclear theory: *from nucleons to stars*

EMERGENT GEOMETRY AND DUALITY IN THE ^{24}MG NUCLEUS

Laboratoire de Physique des 2 infinis Irène Joliot-Curie

Gianluca Stellin

Post-doctorant | Pôle théorie | CNRS UMR 9012

Pièce A239, Bât. 100, IJCLab, Université Paris-Saclay

Orsay, 13th November 2025

Motivation

This self-conjugate magnesium isotope is of astrophysical importance, namely in stellar nucleosynthesis within massive stars ($\gtrsim 8M_\odot$).

Its production though α-particle capture is triggered by the photo-disintegration of ^{20}Ne into ^{16}O + ^{4}He. Secondary sources of ^{24}Mg are also $4 \div 8M_\odot$ stars.

Collaborators: Timo A. Lähde (FZ Jülich, Germany), S. Elhatisari (King-Fahd University, Dhahran, KSA), Shihang Shen and Yabin Wang (Beihang University, China)

Tool: *Nuclear lattice effective field theory* (NLEFT), based on the *auxiliary-field Monte-Carlo* method (AFMC) with Wigner-SU(4)-symmetric interactions plus the Coulomb potential and the *pinhole* algorithm

Why duality? Twofold interpretation of the nuclear eigenfunctions: as correlated A-nucleon states and α-cluster states

Objectives:

- Study the structure of the ground state of the ^{24}Mg nucleus;
- Accessing the low-energy excitations and computing the charge radius, the M1 and E2 moments and the reduced electric and magnetic multipole transition probabilities;
- Test the structure predictions of other approaches, such as *antisymmetrized molecular dynamics* (AMD), the semimicroscopic algebraic cluster model (SACM), the *geometric α-cluster model* (GαCM) and the *ab-initio* projected generator coord. method (PGCM).

J. Cseh et al., *Phys. Rev. C.* ***48****, 1724* (1993)
Y. Kanada-En'yo et al., *Phys. Rev. C.* ***103****, 024603* (2021)
Y. Chiba et al., *Phys. Rev. C.* ***91****, 024317* (2020)
M. Kimura et al., *Prog. Theor. Phys. Suppl.* ***196****, 176-183* (2012)
A. Porro et al., *ArXiv:2407.01325* (2024)
G.S. et al. (subm. to the J. Phys G), *ArXiv:2412.17782* (2024)
G.S. et al. (Heron Press, Sofia), *ArXiv:2510.24522* (2025)

- Investigate the strcuture of Hoyle-state candidates in ^{24}Mg.

J. Cseh et al., *ArXiv:2312.08318* (2023)

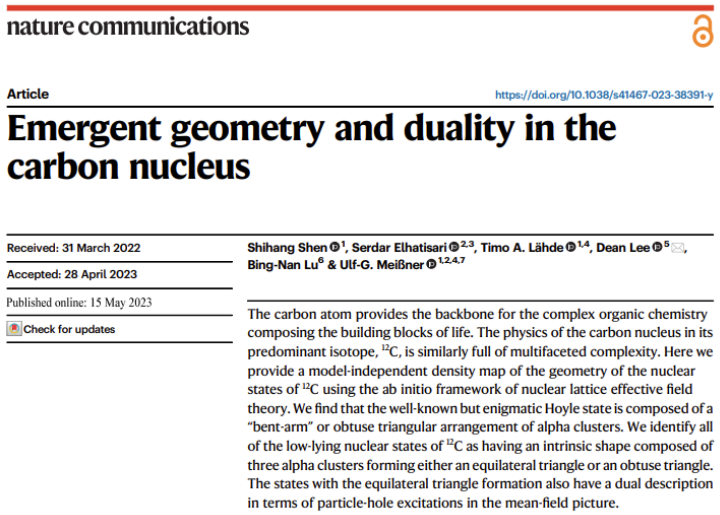

nature communications

Article

https://doi.org/10.1038/s41467-023-38391-y

Emergent geometry and duality in the carbon nucleus

Received: 31 March 2022
Accepted: 28 April 2023
Published online: 15 May 2023
Check for updates

Shihang Shen[1], Serdar Elhatisari[2,3], Timo A. Lähde[1,4], Dean Lee[5], Bing-Nan Lu[6] & Ulf-G. Meißner[1,2,4,7]

The carbon atom provides the backbone for the complex organic chemistry composing the building blocks of life. The physics of the carbon nucleus in its predominant isotope, ^{12}C, is similarly full of multifaceted complexity. Here we provide a model-independent density map of the geometry of the nuclear states of ^{12}C using the ab initio framework of nuclear lattice effective field theory. We find that the well-known but enigmatic Hoyle state is composed of a "bent-arm" or obtuse triangular arrangement of alpha clusters. We identify all of the low-lying nuclear states of ^{12}C as having an intrinsic shape composed of three alpha clusters forming either an equilateral triangle or an obtuse triangle. The states with the equilateral triangle formation also have a dual description in terms of particle-hole excitations in the mean-field picture.

[S. Shen et al., *Nature Comm.* ***14****, 2777* (2023)]

Theoretical framework

NLEFT is a microscopic approach to Schrodinger's A-body problem, representing as a lattice implementation of *ab-initio* Quantum Monte-Carlo methods.

H.-M. Müller et al., *Phys. Rev. C* ***61***, 044320 (2000) D. Lee et al., *Phys. Rev. C* ***70***, 014007 (2004) B. Borasoy et al., *Nucl. Phys. A* ***768***, 179 (2004) B. Borasoy et al., *Eur. Phys. J. A* ***31***, 105 (2007)

Features:

- Nucleons are immersed in a discrete cubic configuration space with volume L^3 where $L = a\,N$ and $N \rightsquigarrow$ number of mesh points per dimension ($= 10$ in the present application).

  $\Rightarrow$ upper cutoff in momentum space: $a = 1 \ldots 2$ fm $\rightarrow p_{\max} = 315 \ldots 630$ MeV

  $\Rightarrow$ periodic boundary conditions do apply for wavefunctions!

- The time axis is also discretized and multiplied for convenience by the imaginary unit ($\rightsquigarrow$ *Euclidean* time)

  $\Rightarrow$ in the temporal direction, boundary conditions for the wavefunctions are antiperiodic ($\rightsquigarrow$ fermions)

- In Wigner SU(4)-symmetric applications, the interactions incorporate smeared contact potentials, with the addition of the Coulomb force, V_{Coul}. The Hamiltonian reads:

$$H = T + V_{2N}^{\mathrm{SU}(4)} + V_{3N}^{\mathrm{SU}(4)} + V_{Coul}$$

where $V_{2N}^{\mathrm{SU}(4)} = \frac{C_2}{2!}\sum_{\mathbf{n}} :\tilde{\rho}(\mathbf{n})^2:$ and $V_{3N}^{\mathrm{SU}(4)} = \frac{C_3}{3!}\sum_{\mathbf{n}} :\tilde{\rho}(\mathbf{n})^3:$ and $\tilde{\rho}(\mathbf{n}) = \sum_i \tilde{a}_i^\dagger(\mathbf{n})\tilde{a}_i(\mathbf{n}) + s_L \sum_i \sum_{|\mathbf{n}'-\mathbf{n}|=1} \tilde{a}_i^\dagger(\mathbf{n}')\tilde{a}_i(\mathbf{n}')$

where C_2 (C_3) are fitted to the *binding energy* (BE) of ^{4}He (^{12}C)

in truly *ab-initio* NLEFT calculations, N^{2}LO interactions from χEFT are adopted ($\approx$ 10x resources needed)

- Suppression of discretization effects, also thanks to the *smeared* second-quantization operators (reduced overbinding):

$$\tilde{a}_i^\dagger(\mathbf{n}) = a_i^\dagger(\mathbf{n}) + s_{NL}\sum_{|\mathbf{n}'-\mathbf{n}|=1} a_i^\dagger(\mathbf{n}') \qquad \text{where } s_L\ (s_{NL}) \text{ are fitted to the } \textit{radius} \text{ (E0 and E2 transition strengths) of } ^{12}\text{C}$$

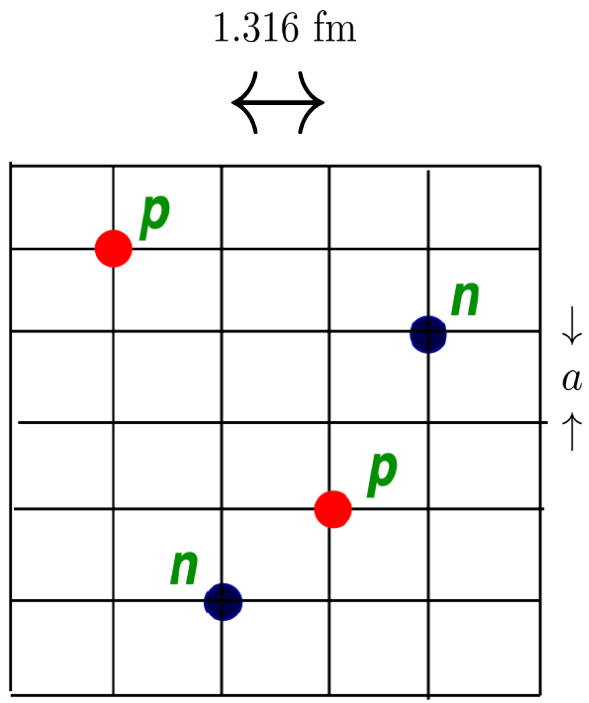

[*Credits*: Timo A. Lähde]

N. Klein et al., *Eur. Phys. J. A* ***54***, 121 (2018)

M. Alarcòn Soriano et al., *Eur. Phys. J. A* ***53***, 83 (2017)

G.S. et al., *Eur. Phys. J. A* ***54***, 232 (2018) , G.S . *PhD thesis* (2020)

N. Li et al., *Phys. Rev. C* ***99***, 064001 (2019)

Adiabatic-projection method

The mechanism underlying NLEFT calculations is stochastic (cf. AFMC) and is based on the *adiabatic projection method*.

D. Lee., *Prog. Part. and Nucl. Phys.* **63**, 117 (2009)

- Let $\tau \equiv it$ be the ***Euclidean time*** interval. From the Hamiltonian, the projected amplitude is defined as: $Z(\tau) = \langle\Phi|\exp(-H\tau/\hbar)|\Phi\rangle$
  where $\exp(-H\tau/\hbar)$ is the time-evolution operator and $|\Phi\rangle$ a trial state
  $\Rightarrow$ discretization of τ into N_t time steps, (Trotter-Suzuki approximation):

$$\begin{array}{c} \tau \mapsto L_t \\ \exp(-H\tau/\hbar) \mapsto M^{N_t} \end{array} \quad \text{where} \quad \begin{array}{c} L_t \equiv N_t\ a_t \\ M \equiv :\exp(-a_t H/\hbar): \end{array}$$

  and M is the ***transfer matrix***. With H in 'lattice units', it becomes $M \equiv :\exp(-\alpha_t H'):$ with $\alpha_t \equiv a_t/a$

- Rationale: in the large-τ limit, the transient energy $E(\tau) = -\hbar\frac{d}{d\tau}\log Z(\tau)$ approaches the energy eigenvalue of the *ground-state* of the Hamiltonian: $E_0 = \lim_{\tau\to\infty} E(\tau)$

  $\Rightarrow$ in practice, when the time axis is discretized, one computes:

$$E_0(L_t) = -\frac{\hbar}{a_t}\log\frac{Z(L_t + a_t)}{Z(L_t)}$$

  and the large-Lt limit is usually reached by means of extrapolation

- For operators $\mathscr{O}$ representing physical observables, one exploits the identities:

$$Z^{\mathscr{O}} \equiv \langle\Phi|e^{-\frac{H\tau}{2\hbar}}\mathscr{O}e^{-\frac{H\tau}{2\hbar}}|\Phi\rangle \quad \text{and} \quad \langle\Psi_0|\mathscr{O}|\Psi_0\rangle = \lim_{\tau\to\infty}\frac{Z^{\mathscr{O}}(\tau)}{Z(\tau)}$$

  where $|\Psi_0\rangle$ is the fully-correlated ground state of the nucleus

  $\Rightarrow$ in lattice calculations, the same observable is calculated through:

$$Z^{\mathscr{O}}(L_t) \equiv \langle\Phi|M^{N_t/2}\mathscr{O}M^{N_t/2}|\Phi\rangle$$

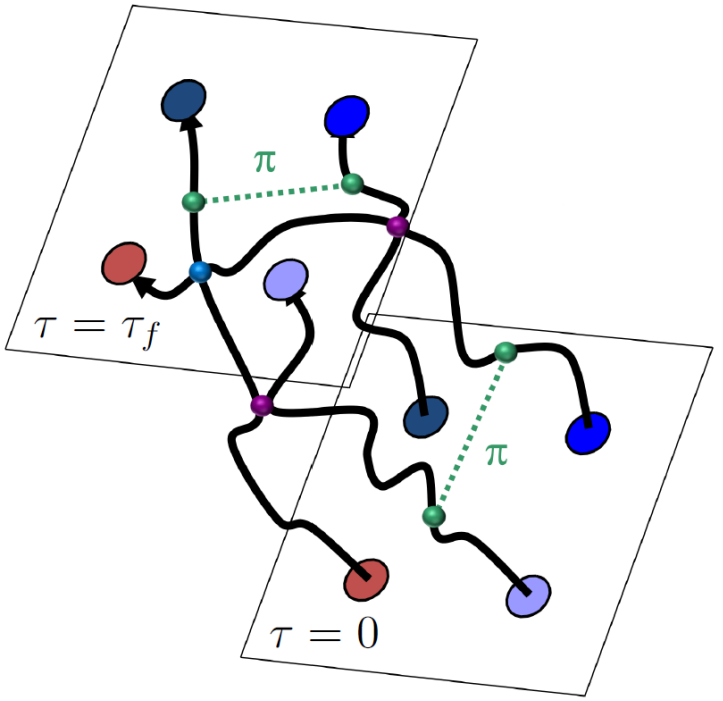

[*Credits*: Timo A. Lähde]

Auxiliary-field Monte-carlo method

- Since NLEFT is a quantum Monte-Carlo (QMC) approach, time-evolution of trial states is achieved by means of a stochastic process.

D. Lee., *Prog. Part. and Nucl. Phys.* **63**, 117 (2009) T.A. Lähde and U.-G. Meißner., *Lecture Notes in Physics.* **957** (2019)

Rationale: decompose the interaction terms of the Hamiltonian into terms which depend linearly on the nucleon fields (cf. the nucl. density), by means of the various formulations of Hubbard-Stratonovich transform performed at every lattice site. In lattice units:

$$\exp\left(-\frac{C'}{2}\rho(\mathbf{n})^2\right) = \frac{1}{\sqrt{2\pi}}\int \mathrm{d}s(\mathbf{n})\ \exp\left(-\frac{s(\mathbf{n})^2}{2} + \sqrt{C'}\rho(\mathbf{n})s(\mathbf{n})\right)$$

C. Körber et al., *Eur. Phys. Lett.* ***119***, *60006* (2017)

where $s(\mathbf{n})$ is an auxiliary field. Meson fields like $\pi(\mathbf{n})$, when present, are treated as auxiliary fields.

- At the end of the tranformation process, amplitudes $Z(L_t)$ become discretized path integrals, taking the form

$$Z(L_t) = \int \mathcal{D}s \int \mathcal{D}\pi\ \langle\Phi|M^{N_t}\{s,\pi\}|\Phi\rangle \equiv \int \mathcal{D}s \int \mathcal{D}\pi\ \det\mathscr{M}\{s,\pi,L_t\}$$

where $\mathscr{M}$ is the *fermion correlation matrix*. The latter is well-defined only for trial states constructed as Slater-determinants of single-nucleon wavefunctions, $|\phi_k\rangle$,

$$\mathscr{M}_{kl}\{s,\pi,L_t\} = \langle\psi_k|M^{N_t}\{s,\pi\}|\psi_l\rangle$$

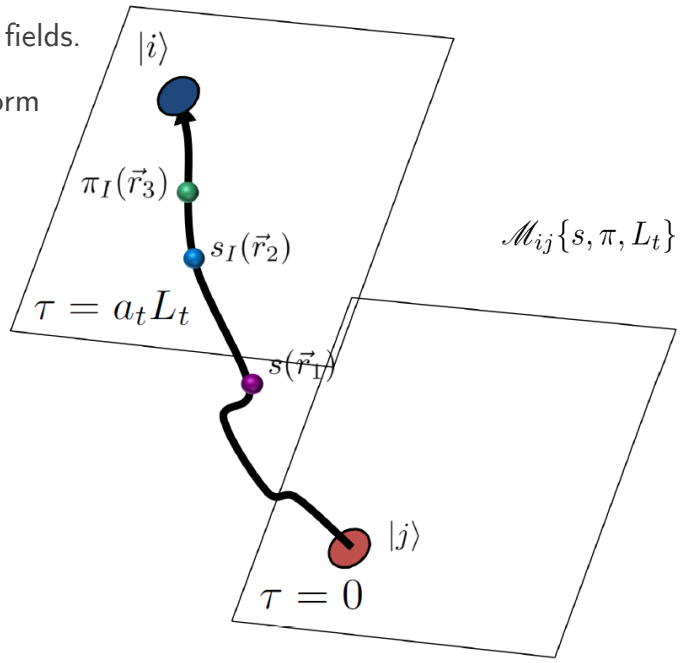

[*Credits*: Timo A. Lähde]

- The auxiliary fields are updated at any Euclidean time slice, following the *Shuttle algorithm*.

Updates are retained or rejected in accordance with the ***Metropolis-Hastings algorithm*** applied to the transfer-matrix products. Issues are encountered whenever the determinant of the fermion correlation matrix oscillates. The «sign» or «phase»-problem is mild when SU(4)-symmetric interactions are adopted.

- The computational requirements scale polinomially with the number of nucleons: $\propto A^{2\div 3}$

Excited states: are obtained through (i) Euclidean time projection with *coupled channels*; (ii) the application of projectors to irreducible representations of point groups (cubic group, $\mathcal{O}$, parity, $\mathscr{P}$, time reversal, $\mathscr{T}$, ...)

Symmetries and trial states

▶ **Trial states:** the available NLEFT code, successfully exploited for ^{12}C (cf. S. Shen et al., *Nature Comm.* ***14***, 2777 (2023)), permits to construct trial wave-functions, $|\Phi\rangle$, of different nature (shell-model, Hartree-Fock, α-cluster ...), with parameters to optimize (HO frequency for shell-model states, α-cluster radii...)

▶ For α-cluster trial wavefunctions, preliminary simulations included the following structures:

Square bipyramid

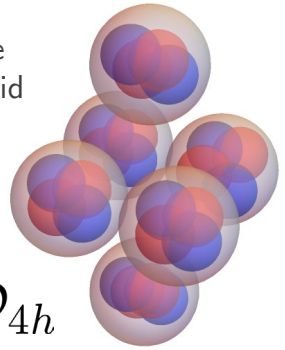

$\mathcal{D}_{4h}$

$\beta_1 = 2.247$ fm
$\beta_2 = 3.566$ fm
$\gamma_1 = 0.0$ rad

fitted to the observed nuclear radius and the E2 moment of the 2_1^+ state

Good prediction of intraband E2 trans. strengths in the GαCM at LO

G.S. et al. (Heron Press, Sofia), *ArXiv:2510.24522* (2025)

Staggered square bipyramid

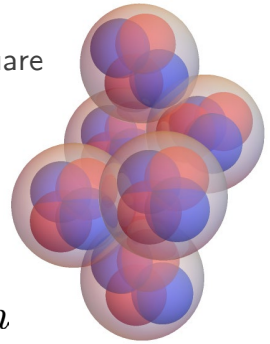

$\mathcal{D}_{2h}$

$\beta_1 = 2.190$ fm
$\beta_2 = 3.010$ fm
$\gamma_1 = 0.5246$ rad

Good prediction of the squared elastic form factor (FF) of the g.s. and the transition FF betw. the 0_1^+ and the 2_1^+ state in the α-particle model in Ref.

R. Bijker et al., *Nucl. Phys. A* ***1006***, 12077 (2021)

with Gaussian charge distribution

Octahedron

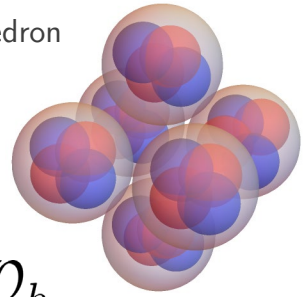

$\mathcal{O}_h$

$\beta_1 = 2.590$ fm
$\beta_2 = 2.590$ fm
$\gamma_1 = 0.0$ rad

The configuration with largest symmetry, perhaps suitable for excited states beyond the g.s. band

Bitetrahedron

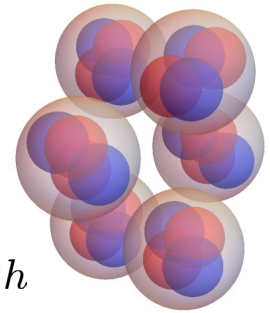

$\mathcal{D}_{2h}$

$\beta_1 = 2.740$ fm
$\beta_2 = 1.650$ fm

Quite good prediction of the experimental squared elastic and transition FFs

P.S. Hauge et al., *Phys. Rev. C* ***4***, 1044 (1971)

▶ Besides, a shell-model trial state with filled harmonic-oscillator (HO) states until the Fermi energy ($1s_{1/2}$ $1p_{3/2}$ $1p_{1/2}$ $1d_{5/2}$) has been constructed

Ground state: Euclidean-time extrapolation

- So far, the five trial-states have been tested for the calculation of the energy eigenvalue of the **ground state**, delivering the binding energy of the nucleus, expected to lie at -198.257 MeV. NLEFT calculations for the 2_1^+ (1.368 MeV), 4_1^+ (4.123 MeV), 2_2^+ (4.238 MeV) and 3_1^+ (5.235 MeV) are ongoing.
- Fitting function for the samples of lattice energy eigenvalues of the g.s. at finite N_t ($\rightsquigarrow$ Euclidean-time extrapolation): $E(N_t) = E_0 + \frac{c_0 e^{-\Delta E_0 N_t}}{1 + c_0 e^{-\Delta E_0 N_t}}(E_0 + \Delta E_0)$

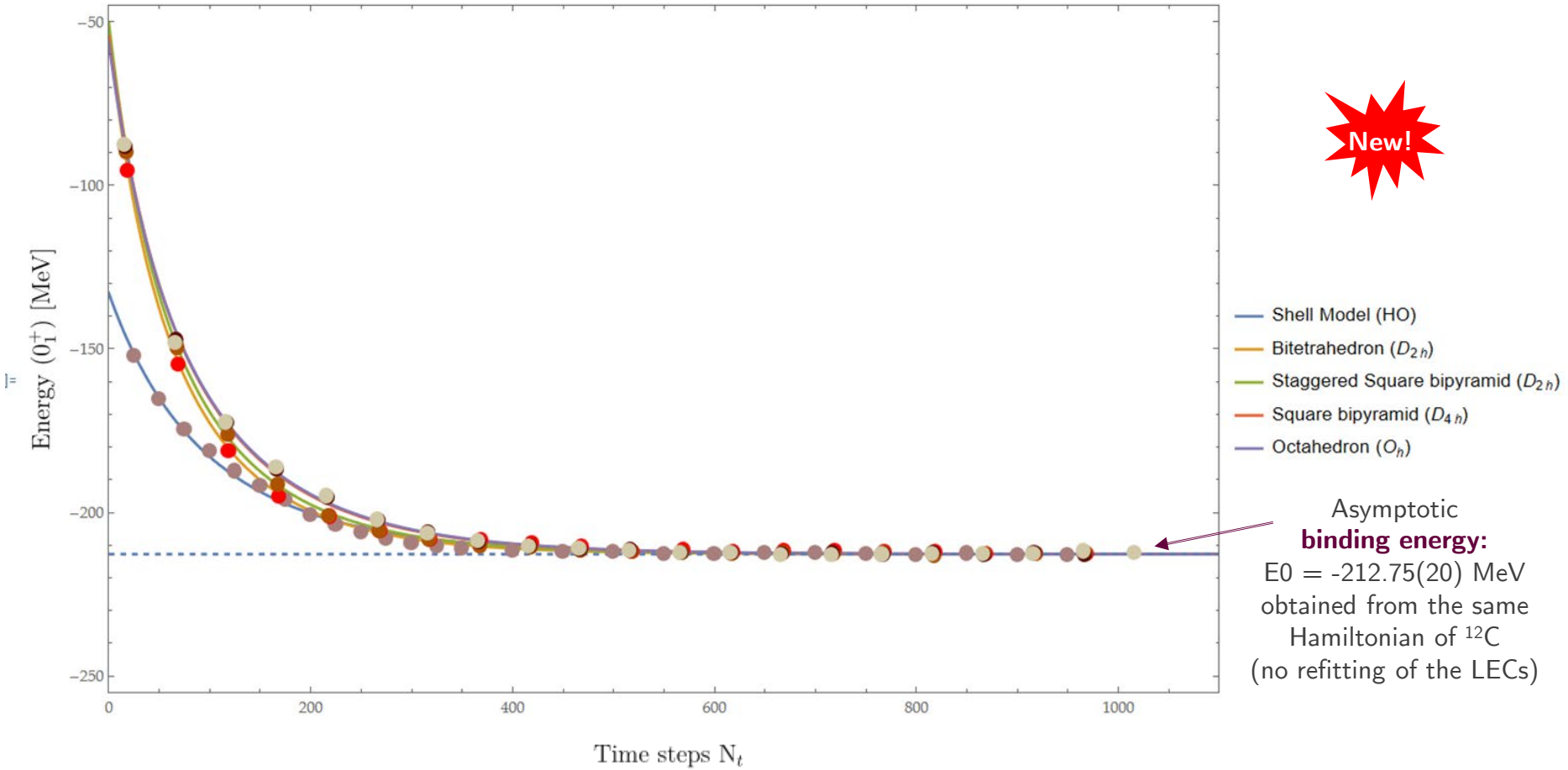

New!

Asymptotic **binding energy:** E0 = -212.75(20) MeV obtained from the same Hamiltonian of ^{12}C (no refitting of the LECs)

Remarks:

Although the sampled shell-model trial state delivers a fitting curve lying below the ones of the considered α-cluster trial states, the former is characterized by a lower convergence rate (ΔE_0= 0.00775(30)) and larger statistical errors than the other states. In particular, for the bitetrahedral trial state one obtains the fastest convergence rate, ΔE_0= 0.00775(30), 0.01030(13), followed by the staggered bipyramidal one, ΔE_0= 0.00934(15), the square bipyramidal one, ΔE_0= 0.00875(15), and the octahedral one, ΔE_0= 0.00842(14).

Lowest 2^+ state: Euclidean-time extrapolation

- So far, the five trial-states have been tested for the calculation of the energy eigenvalue of the **ground state**, delivering the binding energy of the nucleus, expected to lie at -198.257 MeV. NLEFT calculations for the 2_1^+ (1.368 MeV), 4_1^+ (4.123 MeV), 2_2^+ (4.238 MeV) and 3_1^+ (5.235 MeV) are ongoing.

- Fitting function for the samples of lattice energy eigenvalues of the 2_1^+ at finite N_t ($\rightsquigarrow$ Euclidean-time extrapolation): $E(N_t) = E_0 + \frac{c_0 e^{-\Delta E_0 N_t}}{1 + c_0 e^{-\Delta E_0 N_t}}(E_0 + \Delta E_0)$

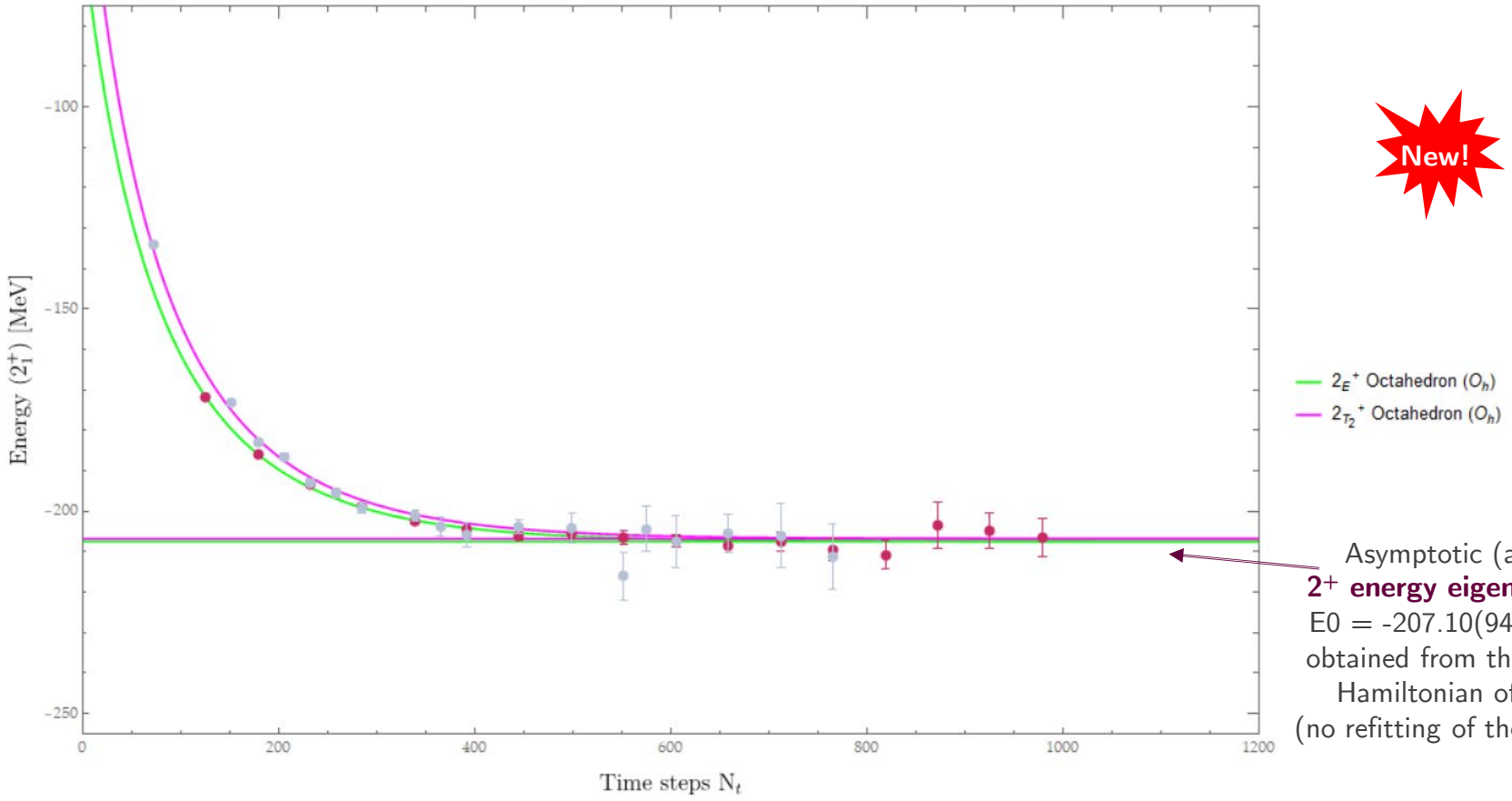

New!

Asymptotic (avg) **2^+ energy eigenvalue:** E0 = -207.10(94) MeV obtained from the same Hamiltonian of ^{12}C (no refitting of the LECs)

Remarks:
The sample for the shell-model trial state is not ready for comparison yet. The considered α-cluster trial state, corresponding to an octahedral equilibrium configuration, has been exploited for both the «E» and the «T_2» irreducible representations of the cubic group. The corresponding fitting functions are characterized by a compatible convergence rate, namely ΔE_0= 0.00835(86) and 0.00825(55) for the «E» and the «T_2» multiplets respectively.

THANK YOU *for your attention!*

Appendix: clustering and intrinsic shape of ^{24}Mg

- The ***geometric alpha-cluster model*** (**GαCM**) is a macroscopic approach describing α-conjugate nuclei in terms of N α-partcles rotating and vibrating about their equilibrium positions, sitting at the vertices of a *polyhedral structure*. Equilibrium configurations are characterized by a *point symmetry group* $\mathcal{G}$.

Inspiration: R. Bijker and F. Iachello, *Nucl. Phys. A* **1006**, 122077 (2021) and G. S., L. Fortunato and A. Vitturi, *J. Phys. G.* **43**, 085104 (2016), *ArXiv:* **1512.025123** (2015).

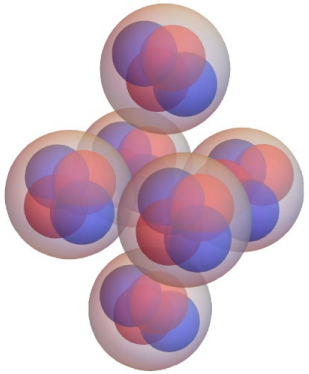

The system is described the quantum vibration-rotation Hamiltonian, with N = 6 α-clusters:

orbital angular momentum — vibrational angular momentum — normal coordinates

$$H = \frac{1}{2}\sum_{\alpha\beta}(J_\alpha - p_\alpha)\mu_{\alpha\beta}(J_\beta - p_\beta) + \frac{1}{2}\sum_{j=1}^{3N-6} P_j^2 + \frac{1}{2}\sum_{j=1}^{3N-6}\lambda_j Q_j^2 - \frac{\hbar^2}{8}\sum_\alpha \mu_{\alpha\alpha}$$

effective reciprocal inertia tensor — conjugate momenta

J.K.G. Watson, *Mol. Phys.* **15**, 479-490 (1968)

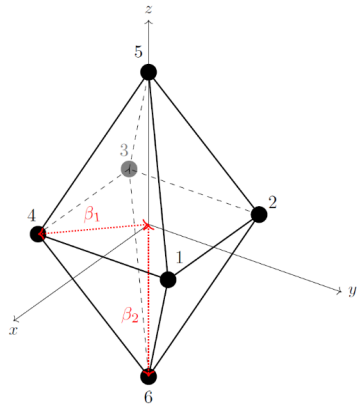

The structure parameters specifying the equilibrium α-configuration are β_1 and β_2.

The model for ^{24}Mg predicts 9 normal modes of vibration, labeled by the irreducible representations of $\mathcal{D}_{4h}$, the symmetry group associated with the intrinsic structure of the nucleus at equilibrium, a **square bipyramid**:

ω_1	ω_2	ω_3	ω_4	ω_5	ω_6	ω_7	ω_8	ω_9	
Q_1	Q_2	Q_3	Q_4	Q_5	Q_6	(Q_7, Q_8)	(Q_9, Q_{10})	(Q_{11}, Q_{12})	
↓	↓	↓	↓	↓	↓	↓	↓	↓	
A_{1g}	A_{1g}	A_{2u}	B_{1g}	B_{2g}	B_{2u}	E_g	E_u	E_u	$\in \mathcal{D}_{4h}$

- The candidates for the 9 rotational bands (singly-excited normal modes) have been *identified* in the measured spectrum!

The exact Hamiltonian can be systematically approximated, by introducing higher-order coupling between rotations an vibrations. At LO rotations and vibrations are decoupled. Thus, the LO Hamiltonian is invariant under *parity*, *time reversal*, and the *equilibrium point group*, $\mathcal{D}_{4h}$.

$$E_{LO}(J,K,[\mathfrak{n}]) = \frac{\hbar^2}{2I_{xx}^{\text{stat}}}[J(J+1)-K^2] + \frac{\hbar^2}{2I_{zz}^{\text{stat}}}K^2 + \sum_{i=1}^{6}\hbar\omega_i(\mathfrak{n}_i+\frac{1}{2}) + \sum_{i=7}^{9}\hbar\omega_i(\mathfrak{n}_i+1) - \frac{\hbar^2}{8}\sum_\alpha I_{\alpha\alpha}^{\text{stat}\,-1}$$

where $(\omega_1,\omega_2,\omega_3,\omega_4,\omega_5,\omega_6,\omega_7,\omega_7,\omega_8,\omega_8,\omega_9,\omega_9) \equiv (\lambda_1,\ \lambda_2\ \ldots\ \lambda_{12})$ ⇝ frequencies of the normal modes

and $\mathfrak{n}_i$ ⇝ number of vibrational quanta of the mode ω_i, vectorized as $[\mathfrak{n}]$

More details:
G.S. et al: ArXiv: **2412.17782** (2024)

Moments of inertia

pointlike charge dristribution:

$$I_{xx}^{\text{stat}} = I_{yy}^{\text{stat}} = 2m(\beta_1^2+\beta_2^2)$$
$$I_{zz}^{\text{stat}} = 4m\beta_1^2$$

Gaussian charge dristribution:

$$I_{xx}^{\text{stat}} = I_{yy}^{\text{stat}} = 2m(\beta_1^2+\beta_2^2) + \frac{6m}{\alpha_1}$$
$$I_{zz}^{\text{stat}} = 4m\beta_1^2 + \frac{6m}{\alpha_1}$$

Adopted values

$(\beta_1, \beta_2) = (2.38, 3.72)$ fm

Appendix: the first excited rotational band B_{2g}

EXAMPLE

Excitation quantum: $\hbar\omega_5 = 2.997(29)$ MeV

associated with the normal coordinate:

$$Q_5 = \sqrt{m}\left(-\frac{\Delta x_1}{2\sqrt{2}} + \frac{\Delta x_2}{2\sqrt{2}} + \frac{\Delta x_3}{2\sqrt{3}} - \frac{\Delta x_4}{2\sqrt{3}} + \frac{\Delta y_1}{2\sqrt{2}} + \frac{\Delta y_2}{2\sqrt{2}} - \frac{\Delta y_3}{2\sqrt{2}} - \frac{\Delta y_4}{2\sqrt{2}}\right)$$

The $K^\pi = 2^+$ bandhead is a 2^+ at 4.123 MeV. The composition of the band reflects the literature assignments, corroborated by the NNDC. It is the most consolidated singly-excited band.

New!

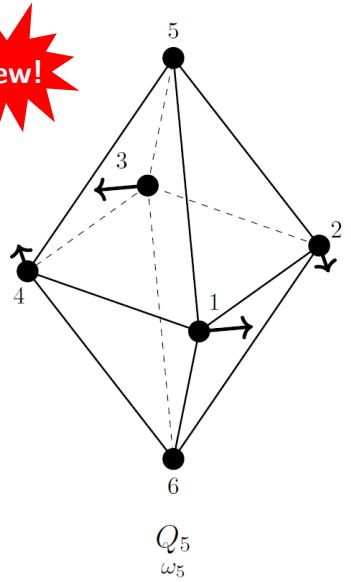

The 6^+ band is a new assignment and rather uncertain.

Description: Symmetric *scissoring mode* of pairs of adjacent α-clusters in the xy plane. The basis of the bipyramid becomes rectangular. The apical α-clusters do not move.

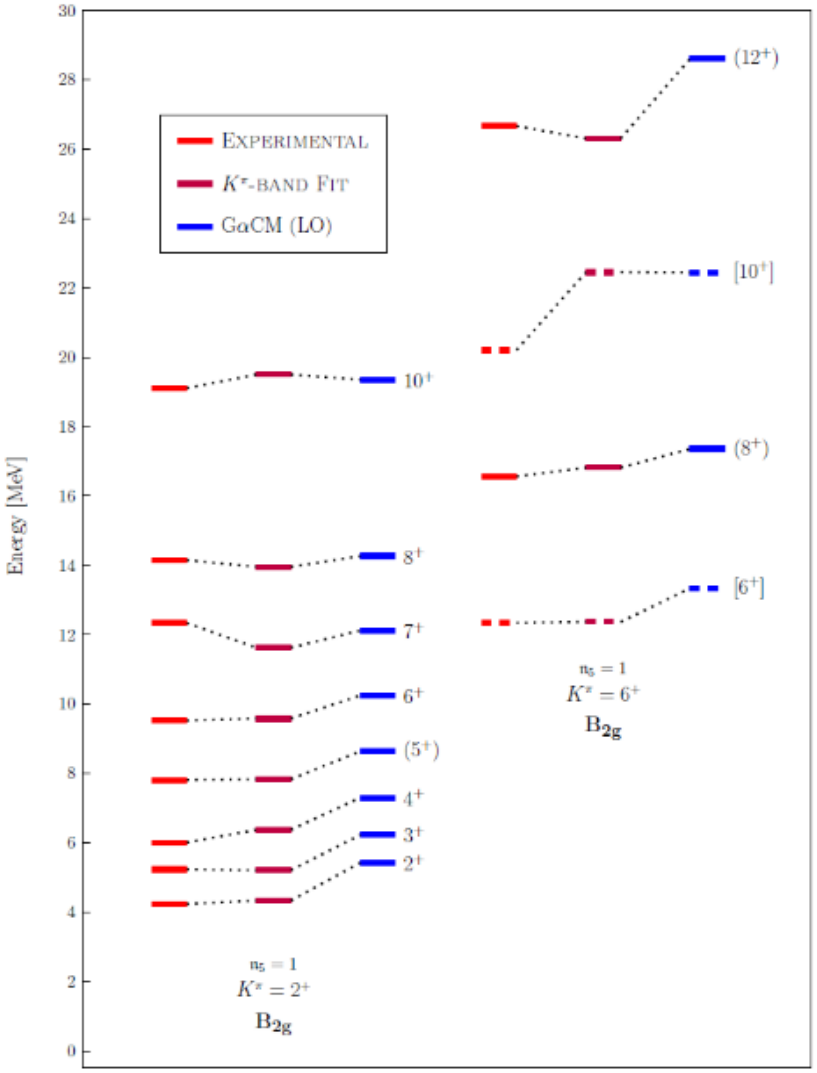

Intraband B_{2g}	Experimental W.U.	Experimental e^2 fm^4	GαCM LO e^2 fm^4
$B[E2; 2^+ (4.123) \to 3^+ (5.235)]$	n.a.	n.a.	196.85
$B[E2; 2^+ (4.238) \to 4^+ (6.010)]$	26.82^{+216}_{-216}	110.30^{+888}_{-888}	84.36
$B[E2; 4^+ (6.010) \to 6^+ (9.528)]$	36.1^{+317}_{-130}	148.5^{+1307}_{-535}	133.62
$B[E2; 5^+ (7.812) \to 7^+ (12.340)]$	n.a.	n.a.	141.59
$B[E2; 6^+ (9.527) \to 8^+ (14.150)]$	n.a.	n.a.	146.02
$B[E2; 8^+ (14.150) \to 10^+ (19.110)]$	n.a.	n.a.	150.17

- The calculated values of the reduced transition probabilities at LO in the GαCM agree with the experimental values within one standard deviation.

Nucleon mass-specific moments of inertia:

$\mathscr{I}_x = 140.3(15)$ fm^2

$\mathscr{I}_z = 87.7(24)$ fm^2

More details:

G.S. et al: ArXiv: **2412.17782** (2024)

Work in progress:
M1, M2 transitions and calculations at NLO

Light Nuclei Workshop
CEA Paris-Saclay
2024

The **ESNT** workshop coorganized by G.S. last year, together with V. Somà and T. Duguet.